Polymer Degradation and Stability 94 (2009) 1772–1778

Contents lists available at ScienceDirect

Polymer Degradation and Stability

journal homepage: www.elsevier.com/locate/polydegstab

Effects of stress ratio on fatigue crack growth of thermoset epoxy resin

C. Kanchanomai*, A. Thammaruechuc

Department of Mechanical Engineering, Faculty of Engineering, Thammasat University, Klong-Luang, Pathumthani 12120, Thailand

ARTICLE INFO

Article history:
Received 8 April 2009
Received in revised form
10 June 2009
Accepted 12 June 2009
Available online 23 June 2009

Keywords:
Epoxy resin
Fatigue crack growth
Cyclic dependence
Time dependence
Creep effect

ABSTRACT

The influences of stress ratio (R) on fatigue crack growth (FCG) of thermoset epoxy resin with polyamine hardener were investigated. The FCG growth rates (da/dN) have been correlated by the linear-elastic fracture mechanics parameters (ΔK and K_{max}), and nonlinear-elastic fracture mechanics parameter (ΔJ). The effects of R on FCG were observed when the ΔK and ΔJ were used as fracture mechanics parameters for FCG. However, the K_{max} successfully characterized FCG under cyclic-dependent condition (FCGs at $R = 0.1$ and 0.4); but it failed to characterize the FCG under time-dependent condition (FCG at $R = 0.7$). As a time-dependent fracture mechanics parameter, C^* was applied to correlate the time-dependent FCG rate (da/dt). A reasonable agreement was obtained between time-dependent FCG ($R = 0.7$) and creep crack growth (CCG) results.

1. Introduction

Epoxy resin generally has low shrinkage after curing, low moisture absorption, wide range of operating temperature (−25 to 150 °C); therefore it has been used as a matrix in various polymer-matrix composites [1–3]. During services, epoxy resins usually perform under cyclic loading at various stress amplitudes and mean stresses. For examples, sport equipment are subjected to low stress amplitudes and low mean stresses; while pressure vessels are subjected to high stress amplitudes and high mean stresses. As a process of defect accumulation, crack initiation, and crack propagation with number of load cycles, the fatigue cracks may initiate and propagate from the discontinuities within a part, i.e. defects during production, cracks during service, or complex geometry of product. The fatigue crack propagation rate depends on various factors, e.g. crack length, stress amplitude, mean stress, frequency, temperature [4].

As a relationship between fracture mechanics parameter and fatigue crack growth rate (da/dN), the fatigue crack growth (FCG) curve could be used in the life prediction of engineering parts under cyclic loading. For linear-elastic materials, the stress intensity factor range (ΔK) could be used to characterize FCG rate; while the range of strain energy released rate (ΔJ) could be used for nonlinear-elastic materials [4]. Since room temperature corresponds to a high homologous temperature for epoxy resin; the time-dependent deformation or creep could become a significant factor in determining the fatigue life. For time-dependent FCG behavior (creep–fatigue interaction), the ΔK and ΔJ are unlikely the appropriate fracture mechanics parameters to crack growth behavior. On the other hand, the time-dependent fracture mechanics parameter (C^*), i.e. a path independent energy rate line integral [5–7], could be used for describing the crack growth rate (da/dt) in both creep-fatigue regime, and creep regime.

Unfortunately, the majority of the FCG studies of polymers have used the linear-elastic fracture mechanics parameters (ΔK and K_{max}) to characterize FCG rates. Ramsteiner and Armbrust [8] studied the FCG of ABS (acrylonitrile-butadiene-styrene) and PMMA (polymethyl methacrylate) using compact-tension (CT) specimens and single edge notch bending (SENB) specimens under stress ratio ($R = K_{min}/K_{max}$) of 0.1. The FCG of both polymers could be characterized by ΔK, and have not influenced by the shape of specimen (CT and SENB) and frequency (1 and 10 Hz). Sadananda and Vasudevan [9] studied FCG of PMMA and polycast PMMA under various R-ratios. They found that crack growth became increasingly dominated by creep process with increasing K_{max}. In contrast, polycast material showed more fatigue damage process (or less of creep-related process) because of its high density of cross-linked chains. Fang et al. [10] studied the FCG behavior of polycarbonate (PC) and acrylonitrile-butadiene-styrene (ABS). They found that the $\Delta K - da/dN$ from low to high crack growth rate could be described with Paris law. Coarse features of porous and dimples have been seen on the crack surfaces with higher crack growth rate; while

* Corresponding author. Tel.: +66 2 564 3001; fax: +66 2 564 3010.
E-mail address: kchao@engr.tu.ac.th (C. Kanchanomai).

0141-3910/$ – see front matter © 2009 Elsevier Ltd. All rights reserved.
doi:10.1016/j.polymdegradstab.2009.06.012

smooth features have been observed on the crack surfaces with lower crack growth rate. A stretched band appears when the crack growth transforms from lower to higher region of FCG rate.

Since the time-dependent deformation or creep of polymer could be a significant factor in determining the fatigue life; it is therefore the purpose of this work to firstly apply nonlinear-elastic fracture mechanics parameters (ΔJ) and time-dependent fracture mechanics parameter (C^*) to characterize FCG rate of polymer. The influences of stress ratio ($R = 0.1$–0.7) on FCGs of thermoset epoxy resin with polyamine hardener were investigated using compact-tension (CT) specimens. The fatigue crack growth rates were characterized by linear-elastic fracture mechanics parameters (ΔK and K_{max}), nonlinear-elastic fracture mechanics parameter (ΔJ), and time-dependent fracture mechanics parameter (C^*). The purely time-dependent crack growth behavior from creep crack growth (CCG) test was also evaluated; and then compared with those of FCG tests. The fracture surfaces as well as replicas of crack tips were investigated using a scanning electron microscope (SEM); and the crack growth processes were then discussed.

2. Material and experimental procedure

Modified liquid epoxy resin (Epotec YD 535 LV) with formulated curing agent (Epotec TH 7257) from Aditya Birla Chemicals (Thailand) Ltd. was used in the present work. The modified DGEBA (diglycidyl ethers bisphenol-A) resin has 172–185 g/eq epoxy equivalent, and <700 g/eq average molecular weight. While, the formulated polyamine hardener has 450–550 mg KOH/g amine equivalent, and comprises of polyamine and cycloaliphatic amine blends. The resin and hardener were initially mixed (100:35 resin/hardener weight ratio), and then cured at ambient temperature for 24 h to the form of flat sheets (10-mm thickness). To achieve the optimum mechanical strength, the post curing was performed in air circulating oven at 80 °C for 4 h.

The elastic shear modulus (G'), viscous shear modulus (G''), and damping coefficient ($\tan\theta = G''/G'$) were obtained using the dynamic mechanical analysis (DMA), as shown in Fig. 1. The tensile test was performed in accordance with the ASTM D638-03 [11]; and the stress–strain relationship is shown in Fig. 2. The uniaxial creep tests were performed in accordance with the ASTM D2990-93 [12]; and the strain–time relationships (creep curves) are shown in Fig. 3. The fracture toughness was obtained from fracture toughness test [13]. The glass-transition temperature was obtained by the differential scanning calorimetry (DSC) technique [14]. The properties of this polymer are summarized in Table 1.

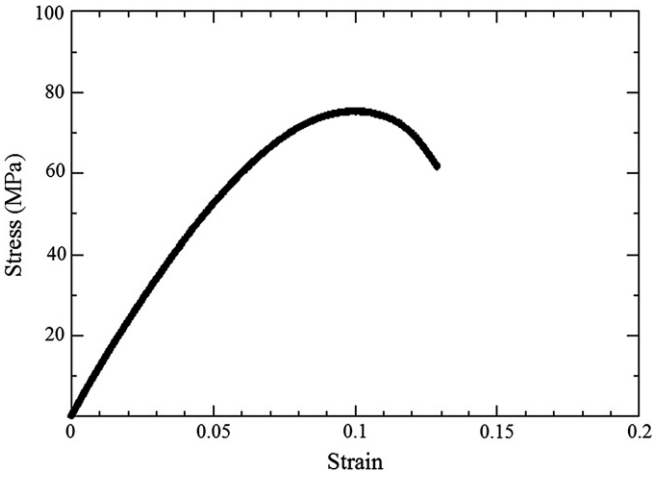

Fig. 2. Stress–strain relationship.

The CT specimens were machined from epoxy resin sheets, and used in the present fatigue crack growth (FCG) tests. The geometry of specimen was in accordance with the ASTM E647-95a [15], as shown in Fig. 4. The notch was introduced by saw machine and a fresh razor blade; and then the pre-crack was introduced by a pre-fatigue test ($\Delta K_o = 0.25$ MPa m$^{1/2}$ and $R = 0.1$). The FCG and CCG tests were performed using a servo-hydraulic fatigue-testing machine (Instron 8872 with 5-kN load cell). The testing environment was air with temperature of 25+/−2 °C and relative humidity of 60+/−5%. A sinusoidal waveform with frequency of 10 Hz, and R-ratios of 0.1, 0.4, and 0.7 were used for the FCG tests. Using a chromel–alumel type thermocouple, the temperatures of CT specimens were measured during FCG tests. The measured temperatures were similar to environment temperature, i.e. 25+/−2 °C. The stress intensity factors (K_o) for CCG tests were in the range of 0.3–0.7 MPa m$^{1/2}$. The crack length (a) was measured by a traveling microscope; while the load-line displacement was measured by a clip gage attached on CT specimen. Both traveling microscope and clip gage have precision of 10 μm. During FCG and CCG tests, the cracks were duplicated using replication technique [16], and observed later under an SEM. After

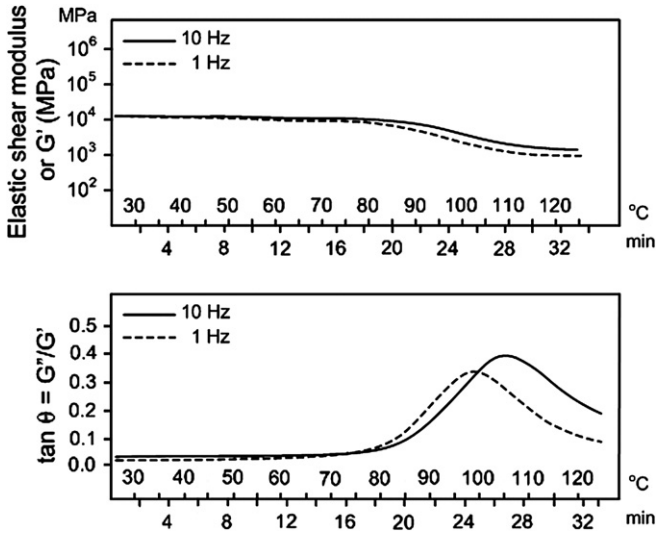

Fig. 1. Elastic shear modulus and damping coefficient.

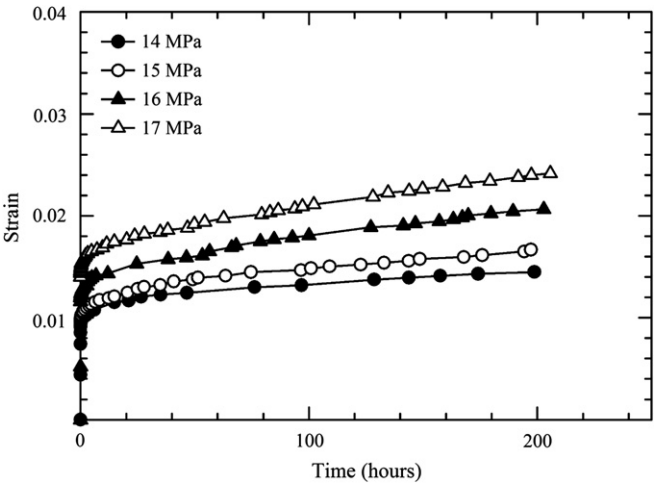

Fig. 3. Strain–time relationships.

Table 1
Properties of epoxy resin.

Glass-transition temperature (°C)	85
Yield stress (MPa)	35
Tensile strength (MPa)	76
Fracture toughness (MPa.m$^{1/2}$)	1.1
Primary creep exponent	5.8
Secondary creep exponent	2.7

failure, the fracture surfaces of FCG and CCG specimens were also observed under an SEM.

As a fracture mechanics parameter for small scale yielding condition, the ΔK can be used for plane-strain FCG if the plastic zone at the crack tip is small compared to crack length, thickness, and uncracked ligament [4].

$$a, B, \quad W - a \; > \; 2.5\left(K_{\max}/\sigma_y\right)^2 \tag{1}$$

where, a is crack length, B is thickness, $W - a$ is uncracked ligament, and σ_y is a yield strength. If the validity of ΔK to FCG rate is confirmed; the ΔK for CT specimen could be calculated as follows [15];

$$\Delta K \; = \; \frac{\Delta P}{B\sqrt{W}} \cdot f(\alpha) \tag{2}$$

$$f(\alpha) = \frac{(2+\alpha)}{(1-\alpha)^{3/2}}\left(0.886 + 4.64\alpha - 13.32\alpha^2 + 14.72\alpha^3 - 5.6\alpha^4\right) \tag{3}$$

where, ΔP is the difference between the maximum and minimum applied loads in a cycle, B is the thickness, W is the width, and α is a/W.

Due to the molecular structure of epoxy resin, nonlinear-elastic deformation is likely to occur; and ΔK may not be an appropriate fracture mechanics parameter. Therefore, the FCG rates were correlated by using ΔJ (a nonlinear-elastic fracture mechanics parameter). The ΔJ was calculated according to the following equation [17];

$$\Delta J \; = \; \frac{2A(1+\beta)}{Bb\left(1+\beta^2\right)} \tag{4}$$

$$\beta \; = \; 2\left[(a/b)^2 + (a/b) + 0.5\right]^{1/2} - 2[(a/b) + 0.5] \tag{5}$$

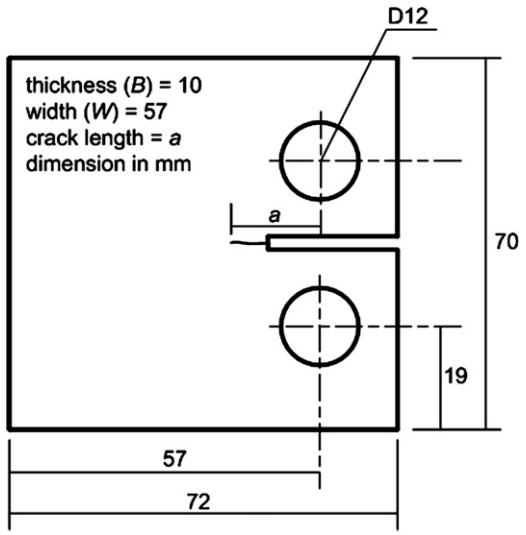

Fig. 4. Geometry of CT specimen.

where, A is the area under the load versus load-line displacement curve, and b is the $W - a$.

Because of the low glass-transition temperature of epoxy resin, the time-dependent deformation or creep is possible for the present environment. Thus, the C^* (which is also known as the creep J-integral or $\dot{J}$) was used to correlated with time-dependent FCG rate (da/dt). The C^* was determined by the following equation [18];

$$C^* \; = \; \frac{P\dot{V}_c}{BW} \cdot \eta \tag{6}$$

$$\eta \; = \; \frac{n}{n+1}\left(\frac{2}{1-\alpha} + 0.522\right) \tag{7}$$

where, P is the applied load ($P_{\max}$ was used for cyclic-loading condition), $\dot{V}_c$ is the upper load-line displacement rate, α is a/W. For FCG tests, n is the primary creep exponent; while n is the secondary creep exponent for CCG test.

3. Results and discussion

3.1. Fatigue crack growth behavior

The FCG rates as a function of ΔK are shown in Fig. 5. The FCG test at $R = 0.1$ exhibited significantly lower FCG rates than those of FCG tests at $R = 0.4$ and 0.7, i.e. FCG curves showed R effect. While the FCG rates of FCG test at $R = 0.4$ were slightly higher than those of FCG test at $R = 0.7$. Above the low crack growth rate region ($da/dN > 10^{-9}$ m/cycle) or Paris regime, the FCG curves exhibited linear relationships between logarithmic da/dN and ΔK, which could be expressed as;

$$da/dN \; = \; C_1(\Delta K)^{m_1} \tag{8}$$

where, C_1 is a constant, and m_1 is the slope on the log–log plot. The C_1 and m_1 for FCG tests at 0.1, 0.4 and 0.7 R-ratios are summarized in Table 2.

As a level of fracture mechanics parameter below which the da/dN becomes very low, the threshold level (ΔK_{th}) for FCG is an

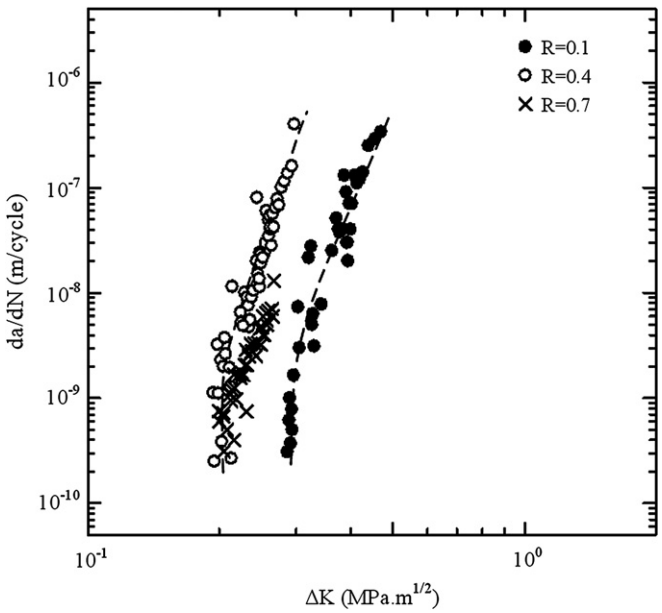

Fig. 5. Relationships between ΔK and da/dN.

Table 2
Fatigue crack growth constants of epoxy resin.

R	ΔK_{th} (MPa.m$^{1/2}$)	ΔJ_{th} (N/m)	$da/dN = C_1\Delta K^{m1}$		$da/dN = C_2\Delta J^{m2}$	
			C_1	m_1	C_2	m_2
0.1	0.30	20.04	1.50×10^{-3}	10.91	3.90×10^{-15}	4.55
0.4	0.20	9.05	1.22	12.86	4.67×10^{-14}	4.84
0.7	0.20	8.89	6.50×10^{-4}	8.57	6.44×10^{-14}	3.37

important characteristic to be considered in assessing the resistance of material to FCG. Although the threshold values at a da/dN of 10^{-11} m/cycle of epoxy resin were not measured; it is still clear from the near-threshold data (Fig. 5) that the ΔK_{th} at $R = 0.1$ was higher than ΔK_{th} at $R = 0.4$ and 0.7. The dependency of FCG rate on R level, when ΔK is used as the correlating parameter, may due to crack closure [4]. A crack closure point could be detected when there is change in linear behavior of the plot between load and load-line displacement during cyclic loading. However, no crack closure was observed for $R = 0.1$, 0.4 and 0.7 FCG tests. The absence of crack closure may due to the flat fracture surface of this polymer.

Since the meaningful crack closure was not present in the tests; the observed R effect must come from some factors other than crack closure. It is known that the ΔK is valid to characterize FCG; if the condition of small scale yielding is satisfied. The calculated plastic zone sizes (Eq. (1)) just before instability crack growth or fast fracture (approximately 23 mm crack length) were 0.35–0.43 mm for FCG tests at $R = 0.1$ and 0.4; while a larger plastic zone of 1.39 mm was found for $R = 0.7$ FCG test. Since all calculated plastic zone sizes were smaller than crack length and uncracked ligament or a small scale yielding condition [4]; it is unlikely that both crack closure and plastic zone size were the reasons for R effect.

It is known that the epoxy resin exhibits nonlinear-elastic behavior [19–21]. Since the nonlinear-elastic behavior increases with increasing load; the R effect may occur when uses linear-elastic fracture mechanics parameter (ΔK) to characterize da/dN of nonlinear-elastic material. Under nonlinear-elastic behavior, the ΔJ is an appropriate fracture mechanics parameter to characterize da/dN. Relationships between ΔJ and da/dN for FCG tests at $R = 0.1$, 0.4 and 0.7 are shown in Fig. 6. The FCG curves using ΔJ showed similar R effect as those using ΔK (Fig. 5). It is unlikely that the nonlinear-elastic deformation behavior was the cause for R effect on FCG behavior of epoxy resin. Although the R effect was observed for $\Delta J - da/dN$ plots; the FCG curves exhibited linear relationships in Paris regime, which could be expressed as;

$$da/dN = C_2(\Delta J)^{m_2} \tag{9}$$

where, C_2 is a constant, and m_2 is the slope on the log–log plot. The C_2 and m_2 for FCG tests at $R = 0.1$, 0.4 and 0.7 are summarized in Table 2.

For ductile fracture, the ΔK is an appropriate fracture mechanics parameter to characterize da/dN. On the other hand, the K_{max} is an appropriate fracture mechanics parameter to characterize da/dN for brittle fracture [22,23]. The FCG rates as a function of K_{max} are shown in Fig. 7. The K_{max} successfully characterized the FCG rate at $R = 0.1$ and 0.4, i.e. both FCG curves located at the same location without the R effect. It is therefore indicated that the FCG behavior at low stress ratios ($R = 0.1$ and 0.4) was brittle manner and cyclic dependence. However, other fatigue mechanisms may occur for FCG test at $R = 0.7$, which exhibited significantly lower FCG rates than those of $R = 0.1$ and 0.4.

3.2. Time-dependent fatigue crack growth behavior

Since the epoxy resin has a low glass-transition temperature; the increase of stress ratio may cause the increasing in time-dependent deformation during FCG test. However, the R effect at $R = 0.1$ and 0.4 was insignificant; and the FCG behavior was cyclic dependence. Under cyclic-dependent condition, the K_{max} could be used to characterize the FCG rates at $R = 0.1$ and 0.4. On the other hand, the contribution of time-dependent deformation on FCG rates may increase, and becomes significant at $R = 0.7$. Under time-dependent FCG, either ΔK, K_{max}, or ΔJ were suitable fracture mechanics parameters for describing the FCG rates.

As a modified J-integral, C^* is the effective fracture mechanics parameter to characterize time-dependent FCG rate. By using the same FCG results, the C^* were determined. The relationships between C^* and da/dt at various R-ratios are shown in Fig. 8. As an indication of purely time-dependent crack growth, the CCG result was also plotted in Fig. 8. If the FCG at $R = 0.7$ is under time-dependent condition; its $C^* - da/dt$ plot would be similar to that of

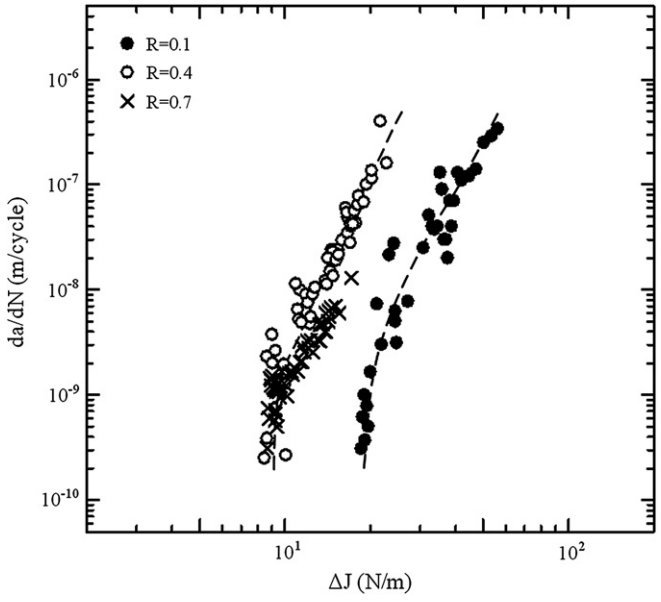

Fig. 6. Relationships between ΔJ and da/dN.

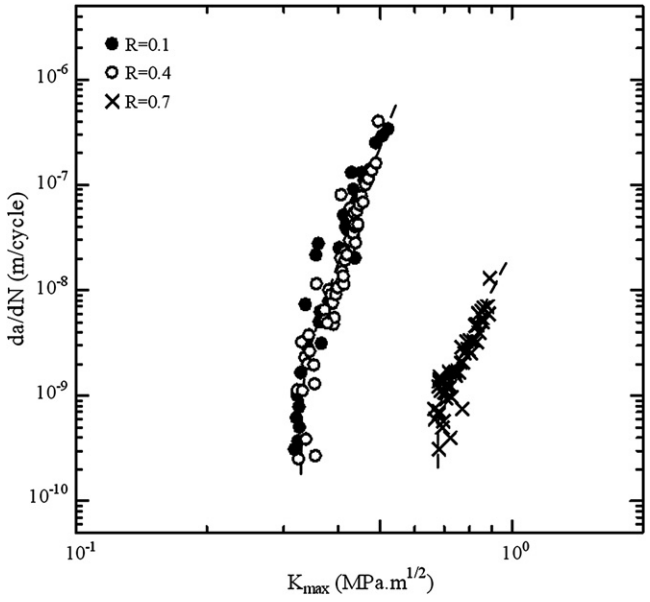

Fig. 7. Relationships between K_{max} and da/dN.

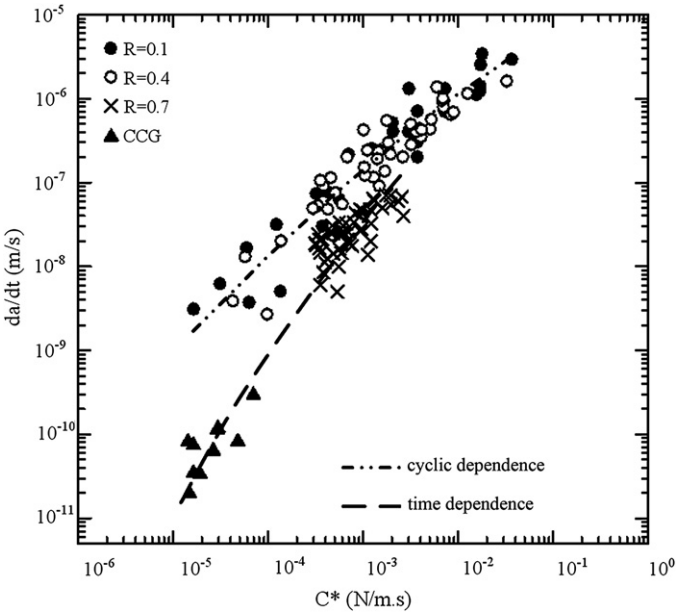

Fig. 8. Relationships between C^* and da/dt.

CCG test. It is noted that the creep crack of epoxy resin propagated in repetitive-stepwise manner; i.e. the radius of crack tip increased with time until some level, crack propagated rapidly, and then stopped. This crack growth process occurred repeatedly during CCG test. Therefore, the time spent during stepwise crack growth process was used in the determination of CCG rate (da/dt).

The $C^* - $ da/dt plots of FCGs at $R = 0.1$ and 0.4 located on the same location at high FCG rates. The difference between the FCG plots ($R = 0.1$ and 0.4) and CCG plot was observed. Together with the finding that the K_{max} successfully characterized the FCG rate at $R = 0.1$ and 0.4; it is therefore confirmed that the FCGs at $R = 0.1$ and 0.4 were under cyclic-dependent condition. On the other hand, the $C^* - $ da/dt plot of $R = 0.7$ FCG shifted to the right or slower FCG rates. Although the CCG rates were approximately two orders lower than the $R = 0.7$ FCG rates; the plots between C^* and da/dt of both $R = 0.7$ FCG test and CCG test showed similar tendency. It is therefore an evidence of the contribution of time-dependent process on $R = 0.7$ FCG. This finding also corresponded to the fact that the plastic zone size of $R = 0.7$ FCG (1.39 mm) was significantly larger than those of $R = 0.1$ and 0.4 FCGs (0.35–0.43 mm).

Generally, C^* is used to describe CCG under static load; while the present work firstly applied C^* to correlate the time-dependent cyclic crack growth of epoxy resin. Although reasonable agreement was obtained between time-dependent FCG and CCG results and it seems that C^* was valid to correlate time-dependent cyclic crack growth of this polymer; further experiments and theoretical work are needed to substantiate it.

3.3. SEM observation

Using replication technique, the crack tips during FCG tests and CCG test have been duplicated, and observed under an SEM. Since the crack tip radii of FCG tests at $R = 0.1$ and 0.4 were similar; only the crack tip radii of FCG tests at $R = 0.4$, 0.7 and CCG were presented here. SEM micrographs of replica films duplicated crack tips of $R = 0.4$ FCG test at $K_{max} = 0.4$ MPa m$^{1/2}$, $R = 0.7$ FCG test at $K_{max} = 0.7$ MPa m$^{1/2}$, and CCG test are shown in Fig. 9. The crack tip radius of FCG test at $R = 0.1$ and 0.4 was small, i.e. cyclic-dependent process. While significantly larger radii of crack tips were observed for $R = 0.7$ FCG and CCG, i.e. evidences of time-dependent process.

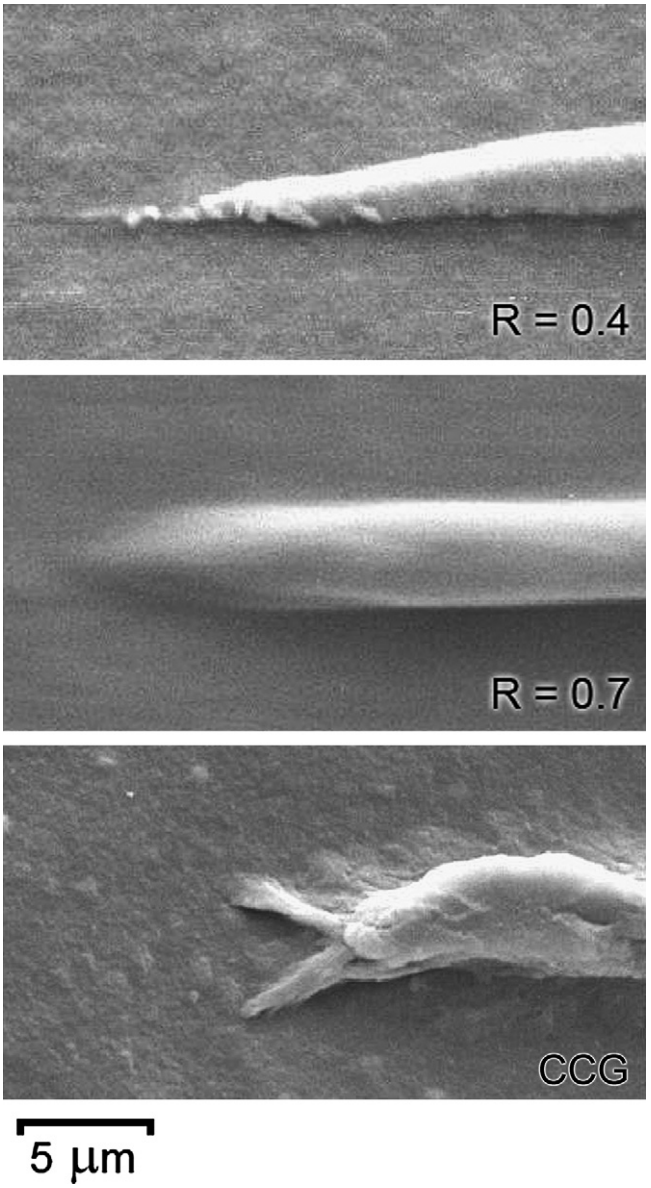

Fig. 9. SEM micrographs of replica films duplicated crack tips of; FCG specimen tested at $R = 0.4$, $K_{max} = 0.4$ MPa m$^{1/2}$, FCG specimen tested at $R = 0.7$, $K_{max} = 0.7$ MPa m$^{1/2}$, and CCG specimen (load direction in vertical).

Crack branching was observed at the crack tip of CCG specimen. This observation corresponded to the formation of shear crazes observed at fatigue crack tip of polyethylene [24]. It is indicated that the creep crack of epoxy resin propagated in repetitive-stepwise manner, i.e. the radius of crack tip increased with time until some level, crack initially propagated in shear mode, turned rapidly to tensile mode, and then stopped. This crack growth process occurred repeatedly during CCG test.

For initially sharp crack, the stress at crack tip theoretically becomes infinite. However this condition is unlikely to occur for real materials; the plastic deformation usually occurs in the vicinity of crack tip, especially in polymers. The plastic deformation at the crack tip results in the increasing of crack tip radius, i.e. crack blunting. At this stage, the stress at crack tip is no longer infinite; and crack growth resistance becomes higher. Since the $R = 0.7$ FCG was influenced by time-dependent process; the radius of crack tip was significantly larger than those of FCG tests at $R = 0.1$ and 0.4 (Fig. 9). This observation corresponded to the finding that the FCG

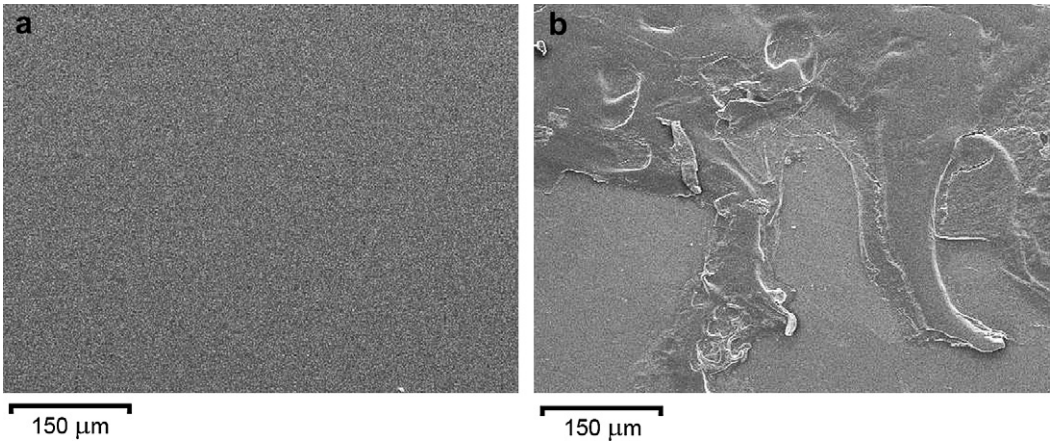

Fig. 10. SEM micrographs of fracture surfaces of; (a) FCG specimen tested at $R = 0.7$, and (b) CCG specimen (crack propagated from right to left).

resistance at $R = 0.7$ was significantly higher than those at $R = 0.1$ and 0.4 FCG tests (Figs. 7 and 8).

Fracture surfaces of the present FCG tests were observed under an SEM. Since the fracture surfaces of FCG tests at $R = 0.1$, 0.4 and 0.7 were similar; only the fracture surface of FCG test at $R = 0.7$ and CCG were presented here (Fig. 10). The FCG specimens ($R = 0.1$, 0.4, and 0.7) exhibited smooth fracture surfaces with 0.06–0.09 μm Ra, i.e. the evidences of fracture without significant plastic deformation or brittle fracture. This observation was in agreement with the finding that no crack closure occurred during FCG tests. On the other hand, evidence of plastic deformation could be seen on the fracture surface of CCG specimen.

Since the FCG at $R = 0.7$ was not purely time-dependent process; but it was an interaction between creep and fatigue. Under this creep–fatigue interaction, both time-dependent and cyclic-dependent processes influenced the crack propagation. For $R = 0.7$ FCG, the time-dependent deformation at crack tip was limited during cyclic loading; thus the ductile fracture could not occur as shown in Fig. 10a. However, the creep–fatigue interaction could enhance the FCG rates; the $R = 0.7$ FCG rates were then faster than the crack growth rates of CCG test (Fig. 8). On the other hand, the CCG was purely time-dependent process; and the time-dependent deformation at crack tip could occur without any influence from cyclic-dependent process. Together with crack branching at the crack tip of CCG specimen (Fig. 9), thus the evidence of ductile fracture was clearly observed as shown in Fig. 10b.

4. Conclusion

The influences of stress ratio (R) on FCG of thermoset epoxy resin with polyamine hardener were investigated. The fatigue crack growth rates were characterized by linear-elastic fracture mechanics parameters (ΔK and K_{max}), nonlinear-elastic fracture mechanics parameter (ΔJ), and time-dependent fracture mechanics parameter (C^*). The findings can be summarized as follows.

1) FCG at $R = 0.1$, 0.4, and 0.7 were under small scale yielding condition without any crack closure. The FCG growth rates (da/dN) could be correlated by ΔK, K_{max}, and ΔJ, i.e. the FCG curves followed Paris's law. The effects of R on FCG were observed when the ΔK and ΔJ were used as fracture mechanics parameters for FCG. However, the K_{max} successfully characterized FCG under cyclic-dependent condition (FCGs at $R = 0.1$ and 0.4); but it failed to characterize the FCG under time-dependent condition (FCG at $R = 0.7$). The FCG resistance at $R = 0.7$ was higher than those of $R = 0.1$ and 0.4 FCG tests. Crack blunting of time-dependent FCG specimen ($R = 0.7$) was the reason of this high FCG resistance.
2) As a time-dependent fracture mechanics parameter, C^* was applied to correlate the time-dependent FCG rate (da/dt). A reasonable agreement was observed between time-dependent FCG ($R = 0.7$) and CCG results. The time-dependent behavior of FCG at $R = 0.7$ was confirmed; and C^* was an appropriate fracture mechanics parameter to correlate time-dependent FCG of epoxy resin.

Acknowledgement

The authors would like to acknowledge the discussions and supports from Professor Y. Mutoh (Nagaoka University of Technology, Japan), Mr. Amit Dixit (Aditya Birla Chemicals (Thailand) Ltd.), the Thailand Research Fund (TRF), the National Research Council of Thailand (NRCT), and the National Metal and Materials Technology Center (MTEC), Thailand.

References

[1] Crawford RJ. Plastics engineering. 3ed. Oxford: Butterworth-Heinemann; 1998.
[2] Margolis JM. Advanced thermoset composites – industrial and commercial applications. New York: Van Nostrand Reinhold; 1985.
[3] Mills NJ. Plastics: microstructure and engineering. 2nd ed. London: Arnold; 1993.
[4] Dowling NE. Mechanical behavior of materials: engineering methods for deformation, fracture, and fatigue. New Jersey: Prentice-Hall International; 1993.
[5] Landes JD, Begley JA. Fracture mechanics approach to creep crack growth. Mechanics of crack growth. ASTM STP 1979;590:128–48.
[6] Ohji K, Ogura K, Kubo S. Estimetes of J-Integral in the general yielding range and its application to creep crack problems. Transaction of JSME 1978; 44(382):1831–8.
[7] Nikbin KM, Webster GA, Turner CE. Relevance of nonlinear fracture mechanics to creep cracking. Cracks and fracture. ASTM STP 1976;601:47–62.
[8] Ramsteiner F, Armbrust T. Fatigue crack growth in polymers. Polym Test 2001;20(3):321–7.
[9] Sadananda K, Vasudevan AK. Analysis of fatigue crack growth behavior in polymers using the unified approach. Mater Sci Eng A 2004;387-389(1–2): 536–41.
[10] Fang QZ, Wang TJ, Li HM. 'Tail' phenomenon and fatigue crack propagation of PC/ABS alloy. Polym Degrad Stab 2008;93(1):281–90.
[11] ASTM D638–03. Standard test method for tensile properties of plastics. In: Annual book of ASTM standards, vol. 8.01; 1994.
[12] ASTM D2990–93. Methods for tensile, compressive, and flexural creep and creep-rupture of plastics. In: Annual book of ASTM standards, vol. 8.02; 1994.
[13] ASTM D5045–93. Standard test method for plane-strain fracture toughness and strain energy release rate of plastic materials. In: Annual book of ASTM standards, vol. 8.02; 1994.
[14] ISO 11357–2. Plastics – differential scanning calorimetry (DSC) – part 2: determination of glass transition temperature; 1999.
[15] ASTM E647–95a. Standard test method for measurement of fatigue crack growth rates. In: Annual book of ASTM standards; 1996.

[16] ASTM E1351–90. Standard practice for production and evaluation of field metallographic replicas. In: Annual book of ASTM standards; 1996.
[17] Clarke GA, Landes JD. Evaluation of the J integral for the compact specimen. J Test Eval 1979;7(5):264–9.
[18] Saxena A. Creep crack growth in high temperature ductile materials. Eng Fract Mech 1991;40(4/5):721–36.
[19] Prosser WH. Ultrasonic characterization of the nonlinear elastic properties of unidirectional graphite/epoxy composites. NASA Contractor Reports 1988.
[20] Kanchanomai C, Rattananon S, Soni M. Effects of loading rate on fracture behavior and mechanism of thermoset epoxy resin. Polym Test 2005;24(7): 886–92.
[21] Kanchanomai C, Rattananon S. Effects of loading rate and thickness on mixed-mode I/II fracture toughness of thermoset epoxy resin. J Appl Polym Sci 2008;109(4):2408–16.
[22] Kujawski D. A fatigue crack driving force parameter with load ratio effects. Int J Fatigue 2001;23(Suppl. 1):239–46.
[23] Dinda S, Kujawski D. Correlation and prediction of fatigue crack growth for different R-ratios using K_{max} and $\Delta K+$ parameters. Eng Fract Mech 2004;71(12):1779–90.
[24] Parsons M, Stepanov EV, Hiltner A, Bear E. Correlation of fatigue and creep slow crack growth in a medium density polyethylene pipe material. J Mater Sci 2000;35:2659–74.